Experimental Validation of Minimum Redundancy Scanning Schemes in PNF Measurements at V band

M.A.Saporetti, L.J. Foged
Microwave Vision Italy (MVI)
Pomezia, Italy
(lars.foged, maria.saporetti)@microwavevision.com

F. D'Agostino, F. Ferrara, C. Gennarelli, R. Guerriero
D.I.In. - Università di Salerno,
84084 Fisciano (SA), Italy
(fdagostino, flferrara, cgennarelli, rguerriero)@unisa.it

D. Trenta
European Space Agency, ESTEC, The Netherlands,
Damiano.Trenta@esa.int

***Abstract*— The planar wide-mesh scanning (PWMS) methodology is based on a non-redundant sampling scheme [1], [2] and is thus without loss of accuracy. It has the potential to enable much faster measurements than standard Planar Near Field (PNF) scanning that is based on denser, regular, equally spaced NF sampling fulfilling Nyquist criteria. In [3], the non-redundant methodology has been validated numerically by simulated measurements on a highly shaped reflector antenna and with actual measurements on a pencil beam antenna in Ku-band and on a navigation antenna in L-band.**

In this paper, we present the experimental verification of the PWMS methodology, at V band using dedicated PNF measurements of a Standard Gain Horn antenna MVG SGH4000.

The results accuracy of the non-redundant methodology has been investigated against Far-Field patterns, implemented by standard scanning methods, by visual comparison, and by computation of the Equivalent Noise Level (ENL). The achieved under-sampling factor is equal to 12, corresponding to similar time reduction in the stepped measurement system employed for the presented validation.

I. INTRODUCTION

In standard Planar Near Field (PNF) systems the radiated near field (NF) from the stationary antenna is measured on a planar surface by a moving probe. The far-field (FF) radiation of the antenna is determined by standard Near-Field to Far-Field (NFFF) transformation [4]. Standard implementations of NF technique are based on dense, regular and equally-spaced NF sampling fulfilling Nyquist criteria.

Much faster measurements can be enabled applying the planar wide-mesh scanning (PWMS) methodology, which is based on a non-redundant sampling scheme [1], [2] and is thus without loss of accuracy.

In [3], the PWMS approach has been applied to two telecommunication Ku-band antennas: the numerical model of a shaped reflector antenna, currently flying on a Eutelsat satellite, and the measurements of a pencil beam multi feed reflector antenna. The non-redundant scanning has been validated also for spherical measurements [5] with a Galileo navigation antenna [6].

In this paper, we present the experimental verification of the PWMS methodology, at V band using dedicated PNF measurements of a standard gain horn MVG SGH4000. Nyquist-compliant and PWMS acquisitions have been performed using a 6 axis Staubli robot.

The results accuracy of the non-redundant methodology will be investigated against Far-Field pattern obtained with Nyquist-compliant measurements, by visual comparison and by computation of the Equivalent Noise Level (ENL) [7]. The actual time-saving, achieved with the PWMS methodology due to the sampling points reduction and sampling path optimization, will be discussed and related to the under-sampling factor.

The paper is organized as follows: In Par. II, the non-canonical scanning and irregular sampling approach for planar NF measurements is shown. Par. III describes the details of the measurements scenario including scanning grid, antenna under test (AUT), and measurement system. In Par. IV, the accuracy of the NFFF transform is assessed by comparing traditional acquisition with fast non-canonical sampling transforms. The results are shown in terms of patterns and Equivalent Noise Level. Finally, the conclusions and future activities are summarized in Par. V.

II. PLANAR WIDE-MESH SCANNING

A non-redundant sampling representation of the voltage, collected through a PWMS NF system on a plane d away from the AUT by a non-directive probe, and the related 2-D optimal sampling interpolation (OSI) expansion [1, 2] are briefly described in the following. The rectangular coordinate system (x, y, z) and the spherical one (r, ϑ, φ), both having their origins O at the AUT aperture center, are introduced to identify a generic observation point, while a point P on the plane can be also specified in the rectangular one (x', y', z') with its origin O' on the scanning plane center (see Figure 1). When using a non-directive probe, the measured voltage has the same effective spatial bandwidth of the electromagnetic (EM) field radiated by the AUT and, according to the non-redundant sampling representations of EM fields [8], it can be approximated with a bandlimited function, provided that a proper surface Σ is adopted to model an electrically large AUT and a suitable parameterization ξ is employed to describe an observation curve on a plane external to Σ. Accordingly, the "reduced voltage" $\tilde{V}(\xi)$, obtained by multiplying the voltage expression V of the probe (V_y) and rotated probe (V_x) by a proper phase factor $e^{j\psi(\xi)}$, is well approximated by a spatially bandlimited function. The resulting bandlimitation error becomes negligible as the bandwidth exceeds a threshold value W_ξ. As a consequence, it can be effectively controlled by choosing a bandwidth equal to $\chi' W_\xi$, $\chi' > 1$ being an enlargement bandwidth factor [8]. When the curve is a radial line, as the x'- (or y'-) axis, the bandwidth W_ξ, the parameter ξ, and the phase function ψ are [1, 2, 8]

$$W_\xi = \beta \ell' / 2\pi; \qquad \xi = (\pi/\ell')\left[R_1 - R_2 + s_1' + s_2'\right] \quad (1)$$

$$\psi = (\beta/2)\left[R_1 + R_2 + s_1' - s_2'\right] \quad (2)$$

where β is the free-space wavenumber, ℓ' the length of C', intersection curve between the surface Σ and the meridian plane through the observation point P, $s_{1,2}'$ the arclength coordinates of the two tangency points $P_{1,2}$ on C', and $R_{1,2}$ the distances from P to $P_{1,2}$. To allow the factorization of the 2-D interpolation algorithm into 1-D OSI expansions along lines, the same optimal parameter ξ or η given by (1) has to be used for all the lines parallel to the x' or y' axis, respectively [1, 2]. Accordingly, the samples on the lines parallel to the x' or y' axis have the same spacings as that relevant to the x' or y' axis (see Figure 1). As regards the phase function ψ, it can be determined [1, 2] by means of (2).

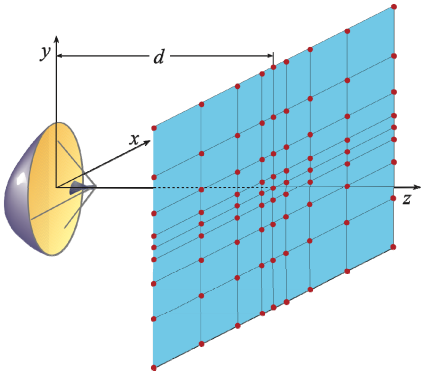

Figure 1. Planar wide-mesh scanning

Since relations (1) - (2) depend on the particular choice of the surface Σ enclosing the AUT and of the observation point, their expressions change accordingly [1, 2]. It is worthy to note that the non-redundant representations adopting the ellipsoidal oblate modelings are simpler than those using the two-bowls ones, since the related expressions are in closed form. On the other hand, the latter are more flexible, since they allow one to better fit antennas having a non-symmetrical extension with respect to the plane identified by their maximum transverse dimension.

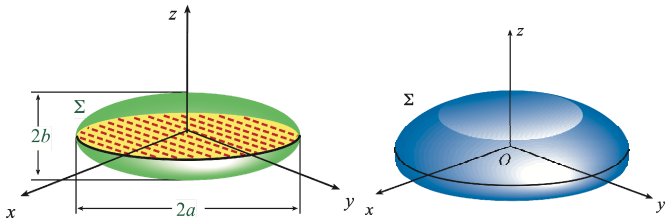

Figure 2. AUT modelings for quasi-planar AUTS: a) oblate ellipsoid; b) two-bowls.

As shown in [1, 2], the following 2-D OSI expansion allows one to accurately evaluate, from the PWMS samples, the voltage $V_{x,y}$ at the points needed by the classical plane-rectangular NFFF falling in the scanning zone:

$$V_{x,y}\left(\xi(x'),\eta(y')\right) = e^{-j\psi(x',y')} \sum_{m=m_0-p+1}^{m_0+p} \left\{ H(\eta,\eta_m,\bar{\eta},N,N'') \cdot \sum_{n=n_0-q+1}^{n_0+q} V_{x,y}(\xi_n,\eta_m)\, e^{j\psi(x_n',\, y_m')} H(\xi,\xi_n,\bar{\xi},N,N'') \right\} \quad (3)$$

where $n_0 = \lfloor \xi/\Delta\xi \rfloor$, $m_0 = \lfloor \eta/\Delta\eta \rfloor$, $2q \times 2p$ is the number of the retained voltages samples $V(\xi_n, \eta_m)$,

$$\xi_n = n\Delta\xi = 2\pi n/(2N''+1); \qquad \eta_m = m\Delta\eta = m\Delta\xi \quad (4)$$

$$N'' = \lfloor \chi N' \rfloor + 1; \qquad N' = \lfloor \chi' W_\xi \rfloor + 1; \qquad W_\eta = W_\xi; \quad (5)$$

$$N = N'' - N'; \qquad \bar{\xi} = q\Delta\xi; \qquad \bar{\eta} = p\Delta\eta \quad (6)$$

$\lfloor x \rfloor$ denotes the greatest integer less than or equal to x, and χ is the OSI oversampling factor required to control the truncation error [8]. Moreover,

$$H(\alpha,\alpha_i,\bar{\alpha},L,L'') = D_{L''}(\alpha-\alpha_i)\,\Omega_L(\alpha-\alpha_i,\bar{\alpha}) \quad (7)$$

is the OSI kernel, $D_{L''}(\alpha)$ and $\Omega_L(\alpha, \bar{\alpha})$ being the Dirichlet and Tschebyscheff sampling functions [8].

III. MEASUREMENT SCENARIO FOR THE VALIDATION

A. *Antenna Under Test*

The AUT is a MVG SGH4000 standard gain horn antenna, shown in Figure 3. The SGH4000 is linearly polarized and is characterized by stable gain with frequency and low return loss / VSWR. It is based on a stiff and robust mechanical design, precision machined with accurate polarization alignment. The dimension of the antenna are 85.x47x38 mm (L x W x H).

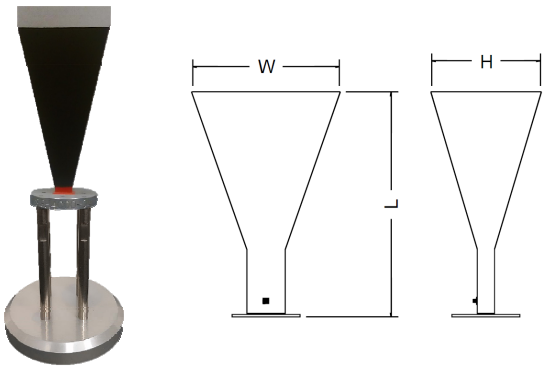

Figure 3. MVI SGH4000

B. *Measurement system*

The measurements have been performed emulating a standard PNF measurement system with a 6 axis Staubli robot, shown in Figure 4. The planar scanning area is 400 x 400 mm in the X-axis (width) and in the Y-axis (height) while, in the Z-axis, the depth is 40 mm. Measurements have been performed using an Open-Ended Waveguide MVG OEW330 (WR229) as probe and with stepped acquisition both in X and in Y axes, at the working frequency of 48 GHz.

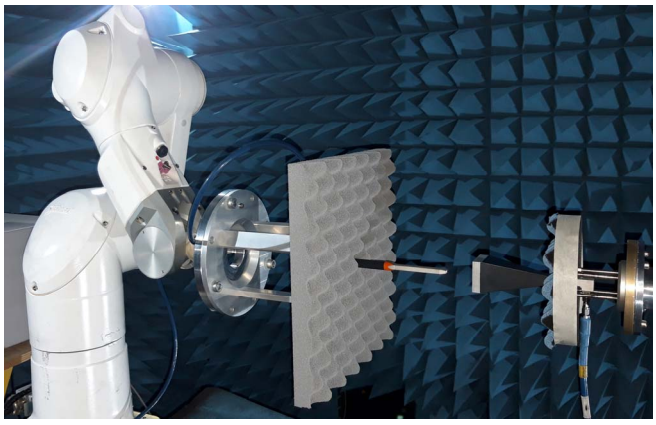

Figure 4. Measurement system with 6-axis Staubli robot, OEW 330 and SGH4000

C. *Scanning grids*

The classical planar NF grid, fulfilling Nyquist criteria (λ/2 sampling step), is constituted by 16641 measurement points, as shown in Figure 5. The acquisition, with the above-mentioned measurement system, has taken 16 hours.

The achievable under-sampling factor in this scenario is equal to 12. The corresponding PWMS grid is constituted by 1369 measurement points distributed uniformly on a grid of 37 x 37 points, as shown in Figure 6. The acquisition has taken 1.5 hours.

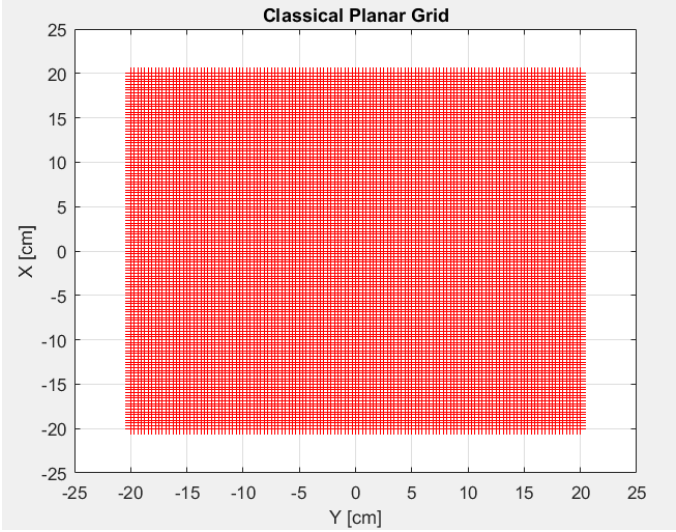

Figure 5. Classical planar NF grid fulfilling Nyquist criteria

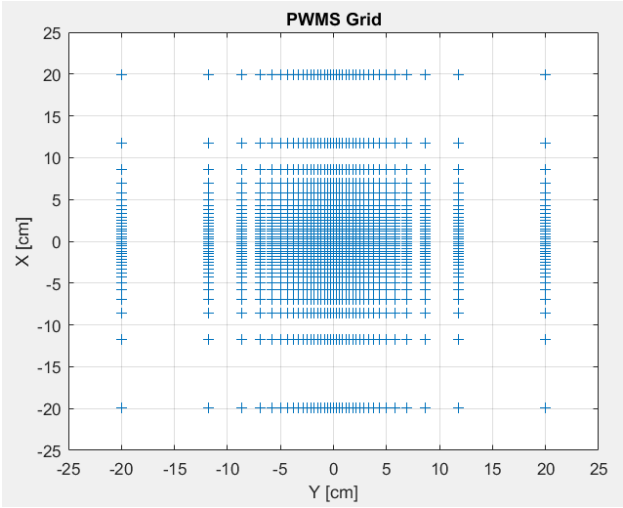

Figure 6. PWMS planar grid with under-sampling factor equal to 12

IV. Validation Results

The results accuracy of the non-redundant methodology has been investigated against FF patterns, implemented by standard scanning methods, by visual comparison, and by computation of the Equivalent Noise Level. Figure 7 and Figure 8 show the isolevel contour shapes, respectively, for the copolar and cross-polar FF components. Figure 9 shows the gain pattern, copolar (solid line) and crosspolar (dashed line) components, of the SGH400 @48GHz in the E-plane.

The blue curve represents the FF obtained with classical Nyquist-compliant acquisition and NFFF transformation. The red curve represents the FF obtained with non-redundant PWMS acquisition, interpolation and NFFF transformation.

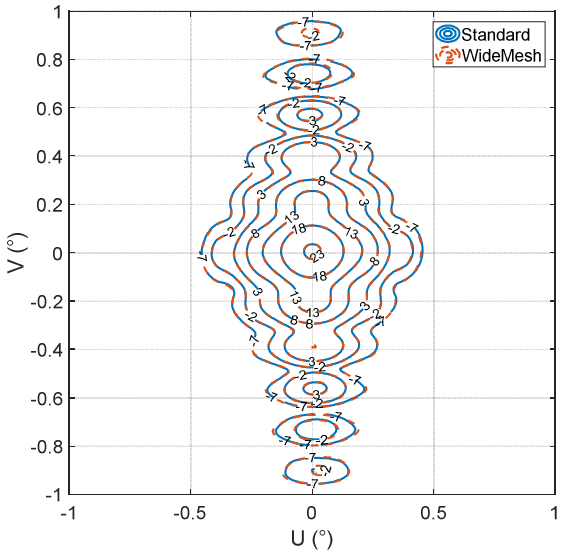

Figure 7. SGH4000 isolevel copolar patterns @48GHz for standard measurement (blue line) and PWMS (red line)

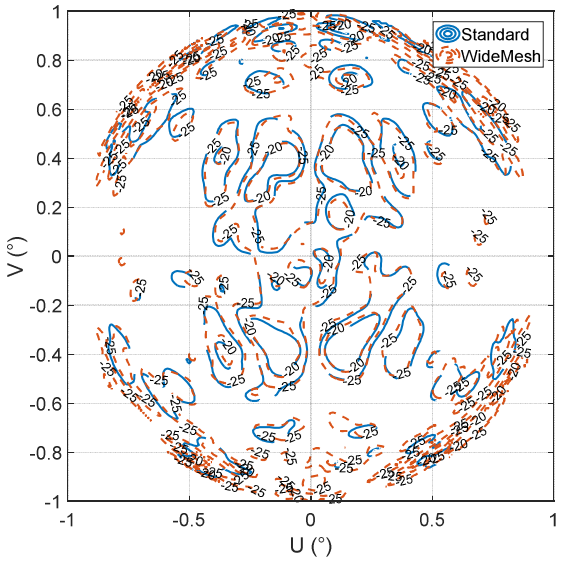

Figure 8. SGH4000 isolevel crosspolar patterns @48GHz for standard measurement (blue line) and PWMS (red line)

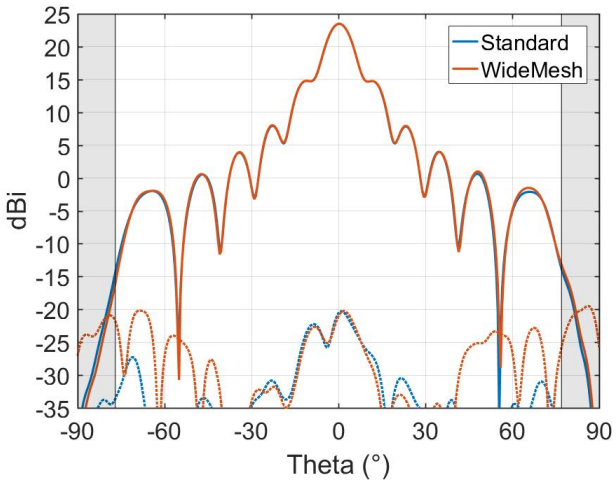

Figure 9. SGH4000 gain pattern @48GHz in the E-plane, copolar (solid curve) and crosspolar (dashed curve) components for standard measurement (blue line) and PWMS (red line)

The shadowed areas in the plot above represent the regions outside the validity angle, computed taking into account the geometrical constraints and which is equal to 78°.

The very good visual agreement of the FF patterns of the non-redundant sampling and the classical NFFF transformation is confirmed by the computed ENL[7] values considering the classical NFFF transformation as reference. The ENL has been computed including all cuts, in a cone with θ ranging in the validity angle. The ENL, considering copolar and crosspolar components, is equal to -55.38 dB.

V. Conclusions

The experimental verification of the PWMS methodology, at V band using dedicated PNF measurements of a MVI SGH4000 standard gain horn has been presented. The measurements have been performed using a 6 axis Staubli robot, which has implemented both the classical Nyquist compliant grid and the non-redundant PWMS acquisition. The NFFF accuracy has been evaluated by comparing traditional technique and PWMS transformations with an under-sampling factor of 12. The very good agreement visible in the presented FF gain patterns, both in the copolar and in the crosspolar components, is confirmed by extremely low levels of Equivalent Noise level, equal to -55.4 dB. This confirms the accuracy for the NFFF transformation from NF points on a non-redundant plane. The time saving is equal to 11 in the measurement system used for the validation, which is stepped in both axes. An additional time reduction factor could be obtained further optimizing the speed of the path and implementing an on-the-fly acquisition.

Acknowledgement

The activities reported in this paper have been partly supported through ESA project “Measurement Methodology For Fast Antenna Testing” and through ARTES by the Italian Space Agency [9].

REFERENCES

[1] F. Ferrara, C. Gennarelli, R. Guerriero, G. Riccio, C. Savarese, "An efficient near-field to far-field transformation using the planar wide-mesh scanning," Jour. Electromagn. Waves Appl., vol. 21, no. 3, pp. 341-357, 2007.

[2] F. D'Agostino, I. De Colibus, F. Ferrara, C. Gennarelli, R. Guerriero, M. Migliozzi, "Far-field pattern reconstruction from near-field data collected via a nonconventional plane-rectangular scanning: experimental testing," Int. Jour. Antennas Prop., vol. 2014, Art. no. 763687, pp. 1-9, 2014.

[3] F. D'Agostino, F. Ferrara, C. Gennarelli, R. Guerriero, M. A.Saporetti, F. Saccardi, L. J. Foged, D. Trenta, "Fast measurement methodology for near field satellite testing," Proc. of EUCAP 2019, Krakow, Poland, Apr. 2019.

[4] IEEE std 1720 "Recommended Practice for Near-Field Antenna Measurements

[5] F. D'Agostino, F. Ferrara, C. Gennarelli, R. Guerriero, M. Migliozzi, "Effective antenna modellings for NF–FF transformations with spherical scanning using the minimum number of data," Int. Jour. Antennas Prop., vol. 2011, ID 936781, 11 pages.

[6] https://www.esa.int/Our_Activities/Navigation/Galileo/Satellite_anat

[7] M.A.Saporetti, L.J. Foged, F. las Heras, A. A. Alexandridis, C. López , I Y. Kurdi, M. Sierra Castañer, International Facility Comparison Campaign at L/C Band Frequencies, AMTA 2017.

[8] O.M. Bucci, C. Gennarelli, C. Savarese, "Representation of electromagnetic fields over arbitrary surfaces by a finite and nonredundant number of samples," IEEE Trans. Antennas Prop., vol. 46, pp. 351-359, March 1998.

[9] ESA Contract No. 4000121164/17/UK/ND, ARTES "MEASUREMENT METHODOLOGY FOR FAST ANTENNA TESTING"